An underdog story: Re-emergence of a polar instability at high pressure in $KNbO_3$

Mohamad Baker Shoker,[1,*] Sitaram Ramakrishnan,[2,*] Boris Croes,[3] Olivier Cregut,[3] Nicolas Beyer,[3] Kokou D. Dorkenoo,[3] Pierre Rodière,[2] Björn Wehinger,[4] Gaston Garbarino,[4] Mohamed Mezouar,[4] Marine Verseils,[5] Pierre Fertey,[5] Salia Cherifi-Hertel,[3] Pierre Bouvier,[2] and Mael Guennou[1,†]

[1] *University of Luxembourg, Department of physics and materials science, 41 rue du Brill, 4422 Belvaux, Luxembourg*
[2] *Institut Néel CNRS/UGA UPR2940, 25 Rue des Martyrs, 38042 Grenoble, France*
[3] *Université de Strasbourg, CNRS, Institut de Physique et Chimie des Matériaux de Strasbourg, UMR 7504, 67000 Strasbourg, France*
[4] *ESRF – European Synchrotron Radiation Facility, 38000 Cedex Grenoble, France*
[5] *Synchrotron SOLEIL, L'Orme des Merisiers, Départementale 128, 91190 Saint-Aubin, France*

(Dated: August 8, 2025)

Ferroelectricity in perovskites is known to be suppressed by a moderate hydrostatic pressure. The notion that a polar instability should reappear in a higher pressure regime is well accepted theoretically but experiments have failed so far to provide a conclusive evidence for it. Here, we investigate a classical but comparatively underlooked ferroelectric perovskite $KNbO_3$. We use single crystal X-ray diffraction, infrared and Raman spectroscopy and second-harmonic generation to explore the phase transition sequence at high pressures up to 63 GPa. We show that the ferroelectric instability manifests itself in the emergence of an incommensurate modulation of the perovskite structure that combines cation displacements and tilts of the oxygen octahedra. Soft modes associated to the tilts and the modulation are clearly observed along with persistent order-disorder signatures. This demonstrates the presence of the high-pressure polar instability in a lead-free perovskite in spite of the centrosymmetric character of all observed high-pressure phases.

Structural instabilities and distortions in perovskite oxides ABO_3 are fundamental to the understanding of their physical and functional properties. They are commonly decomposed in different types based on their symmetry: tilts of the BO_6 octahedra, (anti)polar displacements of the A and B cations and distortions of octahedra. As part of a general effort to understand these instabilities and their interplay in detail, perovskites have been studied under hydrostatic pressure with the aim of formulating general rules governing the behavior of their instabilities, isolated and in combination. For a long time, notably following pioneering work by Samara *et. al.*[1], the common understanding was that those rules were simple: ferroelectric soft modes at the Brillouin zone center should harden under hydrostatic pressure, while soft tilt modes at the zone boundary should soften. Over time, it was realized that the reality is more complex. Tilt instabilities can be in fact either enhanced or suppressed by pressure, as it was confirmed experimentally[2] and subsequently rationalized in several papers refining the general rules with a greater attention to the details of energetics and atomistic interactions[3–5]. As far as ferroelectric instabilities are concerned, it was checked that classical ferroelectric perovskites undergo a ferro- to paraelectric cubic phase transition[6]. In the early 2000s, these views were revisited and challenged by first-principle calculations[7,8] with the key prediction that the ferroelectric soft mode frequency indeed hardens at first, thereby causing a ferro- to paraelectric transition, but then re-soften in a much higher pressure regime, albeit with a drastic change in the phonon eigenvector[9], which should lead to a re-entrance of ferroelectricity.

As the prototypical displacive ferroelectric perovskite with well-documented soft phonon modes at ambient pressure, lead titanate $PbTiO_3$ was the natural contender to check this prediction. Very early on, a combined XRD and Raman spectroscopy study on $PbTiO_3$ at high pressure was reported, claiming evidence for this new high-pressure ferroelectric phase above 50 GPa[10]. However, the evidence came from powder diffraction alone, was particularly fragile and could never be confirmed. In a very recent study[11], second-harmonic generation (SHG) was performed and gave no evidence for a breaking of inversion symmetry up to 90 GPa, leading the authors to conclude on the absence of a high-pressure ferroelectric ground state. Other attempts in other candidate systems in similar pressure ranges ($SrTiO_3$, $CaTiO_3$ etc.)[12,13] have been equally unsuccessful in providing a conclusive proof of this high-pressure ferroelectric soft mode. While this does not invalidate the well-accepted theoretical views, it suggests that re-entrance of ferroelectricity might only happen at much higher pressures where they would have to compete with transition to post-perovskite phases[11] – and where experiments are even more challenging.

In this letter, we investigate the high-pressure behavior of potassium niobate $KNbO_3$. $KNbO_3$ is a classical, lead-free ferroelectric perovskite. It is isostructural to $BaTiO_3$ and is known as a dominantly order-disorder type ferroelectric, where some phonon softening is present but

* These authors contributed equally to this work.
† mael.guennou@uni.lu

incomplete[14]. Its P-T phase diagram up to the paraelectric cubic phase was mapped in details[6]. The persistence of a Raman signal[6] and diffuse x-ray scattering up to at least 26 GPa[15] indicate that Nb local disorder persists even in the cubic phase, which does not make it a priori a favorable ground when looking for ferroelectric soft modes. Yet we will show that the ferroelectric instability indeed reappears under pressure, but has to coexist with the tilt instability that is also favored by pressure.

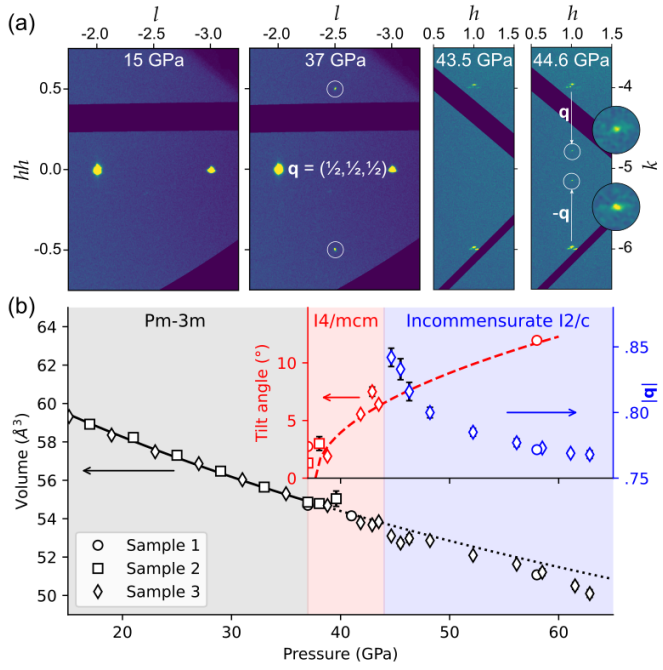

Figure 1. (a) Reciprocal space reconstructions at selected pressures. Circles indicate the positions of the superlattice reflections, commensurate and incommensurate. The reconstructions at 15 and 37 GPa are in the hhl plane with respect to the cubic lattice and the maps at 43.5 and 44.6 GPa in the $hk\bar{1}$ with respect to the tetragonal lattice. (b) Volume, tilt angle and modulation $|\mathbf{q}|$ as a function of pressure. The solid line is a fit to a 2nd-order Birch-Murnaghan equation of state on the cubic volume and the dotted line is its extrapolation. The dashed line for the tilt angle is a guide to the eye.

$KNbO_3$ single crystals grown by the top-seeded solution growth were purchased from SurfaceNet GmbH (Germany) for a series of high-pressure experiments. Experimental details are given in the Supplemental Material[16] (See also Refs.[17–20] therein). All results in the low-pressure range across the ferroelectric to paraelectric transition were found essentially consistent with the literature[6] and will not be shown here. High-pressure single-crystal X-ray diffraction at room temperature were carried out at the SOLEIL synchtrotron source (CRISTAL beamline) and at the ESRF (beamlines ID27[21] and ID15B[22]). At 37 GPa, we observe the appearance of superlattice reflections at commensurate positions $\mathbf{q} = (\frac{1}{2}, \frac{1}{2}, \frac{1}{2})$ (labelled as the R point of the cubic Brillouin zone) as shown in Figure 1. All diffraction maxima were indexed on an I-centered lattice and the structure was successfully described by the space group $I4/mcm$ using the CrysalisPro software package[20] and Jana 2020[23]. It corresponds to the transition to a structure with anti-phase tilts of oxygen octahedra ($a^0a^0c^-$ in Glazer notation[24]). The presence of this phase has not be reported so far in $KNbO_3$, including in a recent powder diffraction study[25], but this occurrence is not surprising. It is pretty ubiquitous in many perovskites, ferroelectric or not ($SrTiO_3$[12], $PbTiO_3$[10], $BaZrO_3$[26], $EuTiO_3$[27]), as a result of a pressure-enhanced instability of this tilt mode at the R point[5]. Complementary DFT calculations of the phonon dispersion (provided in the supplementary information) confirmed that the tilt phonon mode at the R point becomes more and more unstable under pressure, and further preliminary results confirm the stabilization of this tetragonal phase under pressure[28].

At 44.6 GPa, we observed the emergence of incommensurate satellite reflections at $\mathbf{q} = 0.843(7)\mathbf{b^*}$ (Fig. 1(a)). The incommensurate $\mathbf{q}$ was observed to shrink rapidly upon increasing pressure and level off at ≈ 0.77. The superspace approach[29] was employed to elucidate the incommensurate modulation. Initial observation revealed satellites along $\mathbf{a^*}$ and $\mathbf{b^*}$ as shown in the Supplemental Material[16]. However, (3+2)-dimensional (d) modulation was ruled out in favor of (3+1)-d supported by absence of mixed-order satellites. Instead, the satellites along $\mathbf{a^*}$ belong to another domain brought about by the loss of the 4-fold rotational symmetry around $\mathbf{c^*}$. Further evidence proving that the modulated phase is no longer tetragonal arises from the uniaxial direction of the wavevector that is incompatible with the tetragonal ($I4/mcm$) symmetry in (3+1)-d but possible with its orthorhombic and monoclinic subgroups[30]. From structural refinements using Jana 2020[23], a better fit was obtained for a monoclinic superspace group $I2/c(0\sigma_1\sigma_2)0s$ (a-unique ($\sigma_2 = 0$) with $\alpha = 89.40(10)^\circ$) as compared to its orthorhombic supergroup $Ibam(0\sigma0)s00$. A detailed comparison for both models as well as other crystallographic information are provided in the Supplemental Material[16].

An atomistic depiction of the modulation at 58 GPa is given in Figure 2. It is first represented by so-called t-plots showing the amplitude of atomic displacements from the average structure as a function of the phase of the modulation t. Fig. 2(b) shows a pictorial visualization of the modulation by comparing the average structure to the modulated structure at a few selected t values. In addition, a comprehensive visualization of the modulated structure is provided in the form of a movie generated with Jana 2020[16,23]. The modulation appears as quite complex and involves a combination of several distortions. Both K and Nb cations are displaced from their high-symmetry position, thereby breaking inversion symmetry locally. However, Nb is displaced longitudinally along $\mathbf{b}$, i.e. along the modulation vector, while K

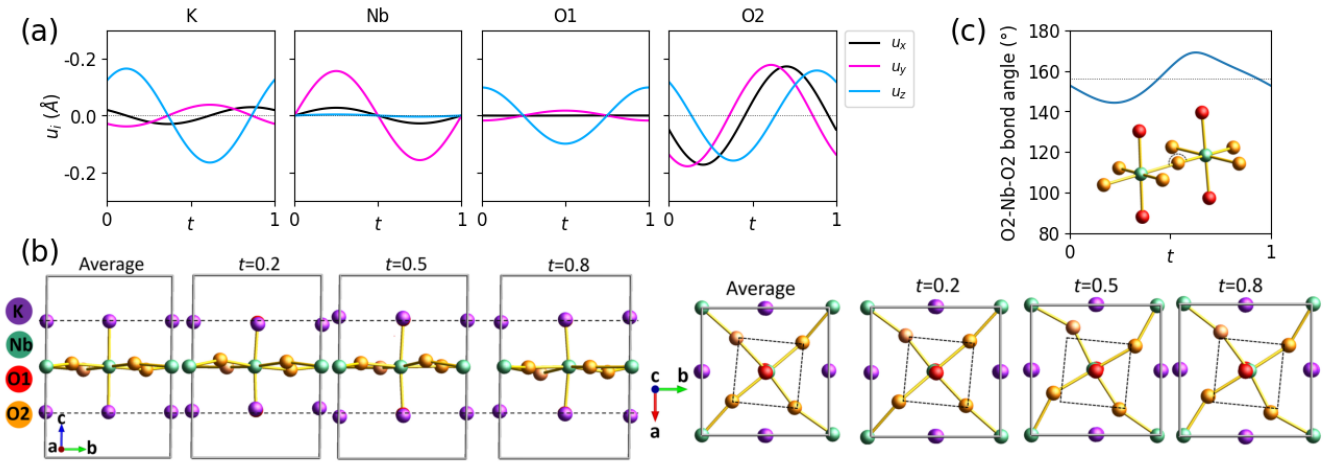

Figure 2. Atomistic depiction of the modulation at 58 GPa (a) t-plots showing all atomic displacements as a function of the phase of the modulation. (b) Projections of the crystal structure of $KNbO_3$ onto the **bc** and **ab** planes at selected t values. Dashed lines serve as a reference to depict the displacement of the atoms from the average structure. (c) Nb-O-Nb bond angle as a function of t. The dashed horizontal line represents the bond angle for the average structure.

(as well as O1) undergo a transverse modulation along **c**. The basal O2 ions appear to be the most heavily modulated in all directions. This can be seen as an *in-phase* tilting motion along the **c** axis that superimposes to the *anti-phase* tilting defining the average $I4/mcm$ structure. This results in a significant modulation of the Nb-O2-Nb bond angle between 169.0(3)° and 144.3(4)° (Fig. 2(c)). Finally, octahedra also undergo stretching along the **c** direction that accompany the K displacements.

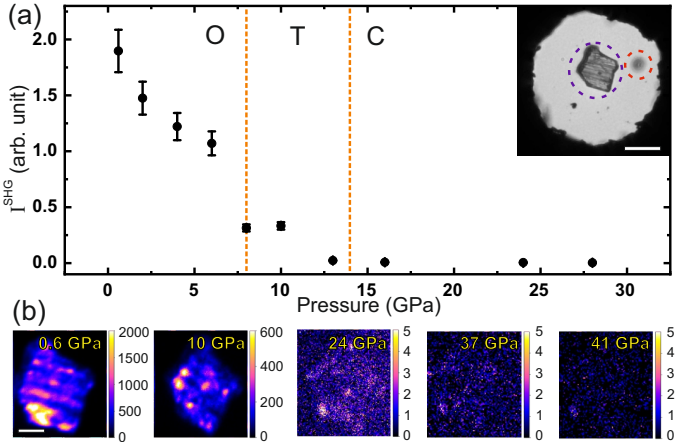

Figure 3. Variation of the second-harmonic generation (SHG) response with pressure. (a) Overall isotropic intensity variation. Dashed lines separate pressure ranges corresponding to the different phases. The inset displays an optical microscopy image showing the sample (blue dashed circle) and the ruby ball (red dashed circle). (b) SHG microscopy images of the sample at selected pressures. The scale bar is 10 µm.

It is sometimes argued that conventional XRD cannot unambiguously determine the presence (or breaking) of macroscopic inversion symmetry and that a dedicated experimental method such as second-harmonic generation (SHG) should be used instead[11]. Indeed, in spite of the use of parameters like Flack, Parsons etc. in modern crystallographic softwares that does allow to distinguish between centrosymmetric and non-centrosymmetric periodic crystals, aperiodic structures can remain problematic. This was illustrated recently with the incommensurate modulation in $EuAl_4$ where the breaking of inversion symmetry was overlooked in a first XRD study[31] before being proposed by SHG measurements[32] and finally corroborated by further diffraction experiments[33]. With this in mind, we performed SHG imaging on a $KNbO_3$ crystal up to 58 GPa. Details are described in the Supplemental Material[16] and Refs.[34,35] therein. The details of the pressure-dependent SHG measurements are described in the supplementary information. As shown in Fig. 3, the SHG intensity averaged over the sample area systematically decreases with increasing hydrostatic pressure. Three distinct regimes can be identified, each corresponding to different phases: $Amm2$ (orthorhombic), $P4mm$ (tetragonal), and ultimately centrosymmetric $Pm\bar{3}m$ (cubic). The corresponding SHG images show a clear domain structure with modulated intensity. At 14 GPa, the intensity drops to essentially zero and didn't show any sign of increase up to the maximum pressure of 58 GPa. Note that the high-pressure cell used for this experiment was the same from which the XRD dataset from Fig 2 was collected, so that there is no doubt that the crystal was in the incommensurate phase, then confirmed to be centrosymmetric.

We now turn to the spectroscopic signatures of the transitions. Raman spectroscopy was performed in several experiments and up to a maximum pressure of 58.1 GPa. The transition to the cubic phase was observed

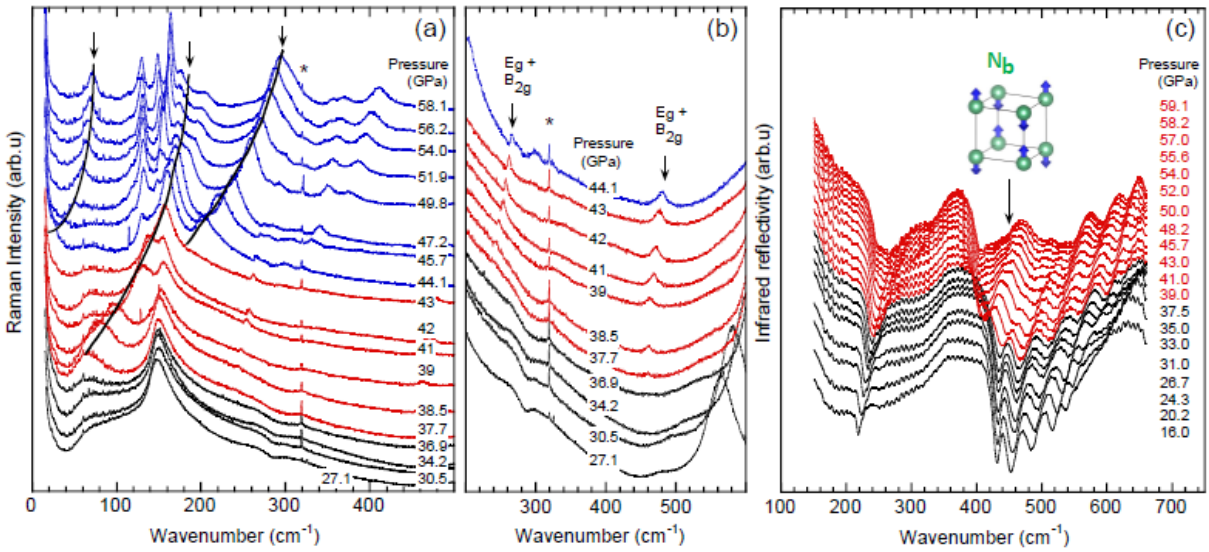

Figure 4. (a) Low-wavenumber Raman spectra showing the different soft modes as discussed in the text. (b) Raman spectra focused on the emergence of the $E_g + B_{2g}$ hard modes associated to the cubic-to-tetragonal transition. (c) Infrared reflectivity spectra. Black, red and blue colors refer to cubic, tetragonal and incommensurate phases respectively. The star * is an artifact.

at 14.3 GPa. Even though no first-order spectrum is allowed by symmetry in a cubic perovskite, the spectrum observed for cubic $KNbO_3$ remains characterized by an intense and structured spectrum shown in the Supplemental Material[16]. This is classically explained by the persistence of local disorder; the Nb^{5+} highly charged d^0 cation is known to stay shifted out of the centers of their octahedra through a pseudo-Jahn–Teller distortion, which occurs when the empty d orbitals form hybrid orbitals with the filled p orbitals of the ligands[36]. Interestingly, this disorder-induced Raman signal weakens but does not vanish with increasing pressure and is still very prominent at 30 GPa at the onset of the antiferrodistortive (AFD) transition, which points to a persistence of the local disorder.

Figure 4 (a) shows the Raman spectra across both high-pressure transitions. Between 37 and 43 GPa, we observe several changes that meet the well-documented expectations for the $Pm\bar{3}m$ to $I4/mcm$ AFD transition[12,26]. This includes the emergence of the soft tilt mode (Fig. 4 (a)) and the activation of hard modes with $E_g + B_{2g}$ symmetry, the splitting of which is allowed by symmetry but negligible in practice[26]. The latter are weak in intensity against the disorder-induced signal, as highlighted in Fig. 4 (b), but their positions match the phonon calculations and their assignment is unambiguous. A much more spectacular change in the Raman signature occurs at 44 GPa with the emergence of the incommensurate modulation. We observe the activation of many sharp hard modes (Fig. 4 (a)). In addition, two modes pointed by arrows in Fig. 4(a) show a pressure hardening akin to soft-mode behavior that we attribute to specific modes named amplitudon and phason that are expected to be activated by the incommensuration[37]. The detailed mode assignment is beyond the scope of this work but we note that the general behavior is compatible with the idea of a change from a phonon density-of-states dominated scattering to a set of discrete lines resulting from the activation of phonons at specific k points. Remarkably, we note that none of the observed soft modes exhibits complete softening, but rather appear at some finite frequency, which is in line with the behaviour of ferroelectric soft modes at ambient pressure and the generally accepted order-disorder character of $KNbO_3$.

Infrared reflectivity spectra were recorded in the same pressure range at the SOLEIL synchrotron source, on a dedicated setup on the AILES beamline[38]. The most prominent signature in the spectra shown in Fig. 4(c) is the activation of a mode located at about 400 cm^{-1} at 37 GPa. Based on calculated phonon frequencies (SI), we attribute this mode to the zone boundary R_4^- mode involving antipolar motions of Nb. This is known and expected from the symmetry lowering from $Pm\bar{3}m$ to $I4/mcm$ but is usually found to be very weak[39]. We speculate that the unusual strength of this mode here may reflect the proximity of the incommensuration and the modulation of the Nb position. In contrast, the activation of the silent T_{2u} (so-called "butterfly") mode of oxygens is not observed, while the weaker signature around 300 cm^{-1} is assigned to the splitting of a polar T_{1u} mode. The transition to the incommensurate phase itself was not observed in that experiment, which we attribute to comparatively poorer pressure condition. Incommensurate phases are known to be fragile against perturbations: suppression of the modulation due to structural defects like dislocations, stacking faults or vacancies has been re-

ported in systems such as $R\mathrm{Te}_3$ (R = rare-earth)[40] and $\mathrm{CuV_2S_4}$[41]. FTIR spectroscopy experiments typically require larger samples that are more susceptible to bridging in the pressure chamber, thereby causing a degradation in crystal quality and a suppression of the modulation. Measurements in this pressure range therefore remain a challenge for state-of-the-art FTIR under pressure.

Incommensurate modulations in simple perovskites are rare but not unheard of. It was proposed that $\mathrm{EuTiO_3}$ shows a modulated structure combining tilts and off-center displacements of Ti along the rotation axis[42,43]. This proposition however was not confirmed by structural refinements, and no such modulation was found under pressure[27]. Much more relevant to the present case are the modulations observed in the model antiferroelectric perovskites $\mathrm{PbZrO_3}$ and $\mathrm{PbHfO_3}$ under pressure[44,45] and recently fully refined in $\mathrm{PbHfO_3}$ as the intermediate phase bridging the paraelectric cubic phase and the $\mathrm{PbZrO_3}$-type commensurate antiferroelectric phase[46]. The modulation in $\mathrm{PbHfO_3}$ shares some similarities with $\mathrm{KNbO_3}$ in that it involves displacements of the A cation as well as additional octahedra tilts. On the other hand, its structure was refined with a higher orthorhombic $Imma(00\gamma)s00$ symmetry, its modulation vector was found to be only weakly temperature-dependent, the intermediate $I4/mcm$ commensurate tilted phase is also not present in $\mathrm{PbHfO_3}$ and the transition mechanism was discussed as triggered rather than soft-mode driven[45], all of which suggest significant differences in the transition mechanisms.

Generally, incommensurate modulations are understood as the result of a tight competition between different instabilities[37]. Here it makes no doubt that the competition between octahedra tilts and a polar instability is the origin of the observed modulation, which in turns demonstrate the re-entrance of the polar instability. The idea of this competition is not new; its basic understanding was substantiated very early on from first principles[47]. However, experimentally, it had led so far to situations where both instabilities are either mutually exclusive, as exemplified by $\mathrm{PbTiO_3}$ where the polar instability needs to be killed first by hydrostatic pressure before the tilt instability can develop[10], or cause transitions to complex structures by convoluted transition mechanisms like in $\mathrm{PbZrO_3}$[48]. The detailed conditions that allow this original phase transition sequence in $\mathrm{KNbO_3}$ will require further theoretical and experimental investigations, but a couple of basic observations can be made. First of all, $\mathrm{KNbO_3}$ has a much larger tolerance factor than $\mathrm{PbTiO_3}$ (1.06 vs. 1.03) which gives the polar instability a head start under pressure. Besides, it is remarkable that this situation is found in a compound with a significant order-disorder character, while other attempts with more displacive compounds were unsuccessfull. This raises the question whether order-disorder might in fact favor such a coexistence. We also note that the modulation in $\mathrm{KNbO_3}$ demonstrates that it does not depend on the presence of Pb or a cation with a lone electron pair. Finally, an obvious open question is whether or not another transition happens in $\mathrm{KNbO_3}$ at even higher pressures above 63 GPa. Even though the modulation vector tends towards $^3/_4$, we anticipate that a true lock-in transition towards a 4-fold superstructure cannot be realized without breaking the I-centering since $4\mathbf{q}$ corresponds to a (030) reflection that is forbidden. Instead, it is tempting to hypothesize that $\mathrm{KNbO_3}$ will undergo a transition to a centrosymmetric, antiferroelectric phase similar to $\mathrm{PbHfO_3}$ and $\mathrm{PbZrO_3}$. This will have to be confirmed experimentally. First-principle calculation will also be instrumental in checking the stability of those phases under pressure.

In summary, we have shown that $\mathrm{KNbO_3}$ exhibits evidence for the re-emergence of a polar instability in the high-pressure regime. Due to the competition with the tilt instability, this polar instability does not give rise to a ferroelectric phase but to a modulated centrosymmetric structure that combines octahedra tilts and polar displacements of both A and B cations. Whether or not a macroscopically polar phase can appear at even higher pressures, in $\mathrm{KNbO_3}$ or in other systems, remains an open question. This calls for an in-depth re-investigation of the pressure-temperature phase diagram of $\mathrm{KNbO_3}$, especially towards the low-temperature region where we might expect an even more intricate competition of ferroelectricity and tilts. The conditions that make this possible in $\mathrm{KNbO_3}$, and specifically the possible role of some order-disorder in balancing the competition between instabilities, will also require theoretical investigations with and beyond standard DFT approaches.

Acknowledgments – The authors thank Philippe Ghosez and Hao-Cheng Thong for helpful discussions on preliminary first-principle calculations as well as Jeroen Jacobs for the preparation of the high-pressure cells and Stany Bauchau for technical support at the ESRF beamline. We acknowledge SOLEIL and the ESRF for provision of synchrotron radiation facilities under proposals N. 20231689, 20241276 and HC-6148 respectively. S.R. and P.R. thank the support from the Agence Nationale de la Recherche under the project SUPERNICKEL (Grant No.ANR-21-CE30-0041-04). We also acknowledge the Interdisciplinary Thematic Institute 2021-2028 and EUR QMat (ANR-17-EURE-0024), as part of the ITI 2021-2028 program supported by the IdEx Unistra (ANR-10-IDEX-0002) and SFRI STRAT'US (ANR-20-SFRI-0012) through the French Programme d'Investissement d'Avenir.

The high-pressure X-ray diffraction data is available at https://doi.esrf.fr/10.15151/ESRF-ES-2107750542.

[1] G. A. Samara, T. Sakudo, and K. Yoshimitsu, Important generalization concerning the role of competing forces in displacive phase transitions, Phys. Rev. Lett. **35**, 1767 (1975).

[2] P. Bouvier and J. Kreisel, Pressure-induced phase transition in $LaAlO_3$, J. Phys.: Condens. Matter **14**, 3981 (2002).

[3] R. J. Angel, J. Zhao, and N. L. Ross, General rules for predicting phase transitions in perovskites due to octahedral tilting, Phys. Rev. Lett. **95**, 025503 (2005).

[4] J. Zhao, N. L. Ross, and R. J. Angel, New view of the high-pressure behaviour of $GdFeO_3$-type perovskites, Acta Crystallographica Section B **60**, 263 (2004).

[5] H. J. Xiang, M. Guennou, J. Íñiguez, J. Kreisel, and L. Bellaiche, Rules and mechanisms governing octahedral tilts in perovskites under pressure, Phys. Rev. B **96**, 054102 (2017).

[6] P. Pruzan, D. Gourdain, and J. C. Chervin, Vibrational dynamics and phase diagram of $KNbO_3$ up to 30 GPa and from 20 to 500 K, Phase Transitions **80**, 1103 (2007).

[7] I. A. Kornev, L. Bellaiche, P. Bouvier, P.-E. Janolin, B. Dkhil, and J. Kreisel, Ferroelectricity of perovskites under pressure, Phys. Rev. Lett. **95**, 196804 (2005).

[8] I. A. Kornev and L. Bellaiche, The nature of ferroelectricity under pressure, Phase Transitions **80**, 385 (2007).

[9] E. Bousquet and P. Ghosez, First-principles study of barium titanate under hydrostatic pressure, Phys. Rev. B **74**, 180101 (2006).

[10] P.-E. Janolin, P. Bouvier, J. Kreisel, P. A. Thomas, I. A. Kornev, L. Bellaiche, W. Crichton, M. Hanfland, and B. Dkhil, High-pressure effect on $PbTiO_3$: An investigation by Raman and x-ray scattering up to 63 GPa, Phys. Rev. Lett. **101**, 237601 (2008).

[11] R. E. Cohen, Y. Lin, M. Ahart, and R. J. Hemley, Absence of high-pressure ground-state reentrant ferroelectricity in $PbTiO_3$, Phys. Rev. Lett. **133**, 236801 (2024).

[12] M. Guennou, P. Bouvier, J. Kreisel, and D. Machon, Pressure-temperature phase diagram of $SrTiO_3$ up to 53 GPa, Phys. Rev. B **81**, 054115 (2010).

[13] M. Guennou, P. Bouvier, B. Krikler, J. Kreisel, R. Haumont, and G. Garbarino, High-pressure investigation of $CaTiO_3$ up to 60 GPa using x-ray diffraction and raman spectroscopy, Phys. Rev. B **82**, 134101 (2010).

[14] M. D. Fontana, G. Metrat, J. L. Servoin, and F. Gervais, Infrared spectroscopy in $KNbO_3$ through the successive ferroelectric phase transitions, Journal of Physics C: Solid State Physics **17**, 483 (1984).

[15] S. Ravy, J.-P. Itié, A. Polian, and M. Hanfland, High-pressure study of x-ray diffuse scattering in ferroelectric perovskites, Phys. Rev. Lett. **99**, 117601 (2007).

[16] See Supplemental Material at [URL will be inserted by publisher] for a) a document containing experimental details as well as complementary results and tables as detailed in the text, and b) a movie representing the modulated structure for t values ranging from 0 to 1 in the **bc** and **ab** planes.

[17] G. Shen, Y. Wang, A. Dewaele, C. Wu, D. E. Fratanduono, J. Eggert, S. Klotz, K. F. Dziubek, P. Loubeyre, O. V. Fat'yanov, P. D. Asimow, T. Mashimo, and R. M. M. Wentzcovitch, Toward an international practical pressure scale: A proposal for an ipps ruby gauge (ipps-ruby2020), High Pressure Research **40**, 299 (2020).

[18] K. Takemura, Evaluation of the hydrostaticity of a helium-pressure medium with powder x-ray diffraction techniques, Journal of Applied Physics **89**, 662 (2001).

[19] A. Dewaele and P. Loubeyre, Pressurizing conditions in helium-pressure-transmitting medium, High Pressure Research **27**, 419 (2007).

[20] Rigaku, CrysAlis Pro Version 171.43.90, Rigaku Oxford Diffraction. (2023).

[21] M. Mezouar, G. Garbarino, S. Bauchau, W. Morgenroth, K. Martel, S. Petitdemange, P. Got, C. Clavel, A. Moyne, H.-P. Van Der Kleij, A. Pakhomova, B. Wehinger, M. Gerin, T. Poreba, L. Canet, A. Rosa, A. Forestier, G. Weck, F. Datchi, M. Wilke, S. Jahn, D. Andrault, L. Libon, L. Pennacchioni, G. Kovalskii, M. Herrmann, D. Laniel, and H. Bureau, The high flux nano-x-ray diffraction, fluorescence and imaging beamline ID27 for science under extreme conditions on the ESRF extremely brilliant source, High Press. Res. **44**, 171 (2024).

[22] G. Garbarino, M. E. Hanfland, S. Gallego-Parra, A. D. Rosa, M. Mezouar, D. Duran, K. Martel, E. Papillon, T. Roth, P. Got, and J. Jacobs, Extreme conditions x-ray diffraction and imaging beamline ID15B on the ESRF extremely brilliant source, High Press. Res. **44**, 199 (2024).

[23] V. Petříček, L. Palatinus, J. Plášil, and M. Dušek, Jana2020 – a new version of the crystallographic computing system Jana, Zeitschrift für Kristallographie - Crystalline Materials **238**, 271 (2023).

[24] A. M. Glazer, Simple ways of determining perovskite structures, Acta Crystallogr. A **31**, 756 (1975).

[25] Y. Kobayashi, S. Endo, T. Ashida, L. C. Ming, and T. Kikegawa, High-pressure phase above 40 GPa in ferroelectric $KNbO_3$, Phys. Rev. B **61**, 5819 (2000).

[26] C. Toulouse, D. Amoroso, R. Oliva, C. Xin, P. Bouvier, P. Fertey, P. Veber, M. Maglione, P. Ghosez, J. Kreisel, and M. Guennou, Stability of the tetragonal phase of $BaZrO_3$ under high pressure, Phys. Rev. B **106**, 064105 (2022).

[27] D. Bessas, K. Glazyrin, D. S. Ellis, I. Kantor, D. G. Merkel, V. Cerantola, V. Potapkin, S. van Smaalen, A. Q. R. Baron, and R. P. Hermann, Pressure-mediated structural transitions in bulk $EuTiO_3$, Phys. Rev. B **98**, 054105 (2018).

[28] P. Ghosez, private communication (2025).

[29] S. van Smaalen, *Incommensurate Crystallography*, International Union of Crystallography Monographs on Crystallography (OUP Oxford, 2007).

[30] H. T. Stokes, B. J. Campbell, and S. van Smaalen, Generation of $(3+d)$-dimensional superspace groups for describing the symmetry of modulated crystalline structures, Acta Crystallogr. A **67**, 45 (2011).

[31] S. Ramakrishnan, S. R. Kotla, T. Rekis, J.-K. Bao, C. Eisele, L. Noohinejad, M. Tolkiehn, C. Paulmann, B. Singh, R. Verma, B. Bag, R. Kulkarni, A. Thamizhavel, B. Singh, S. Ramakrishnan, and S. van Smaalen, Orthorhombic charge density wave on the tetragonal lattice of $EuAl_4$, IUCrJ **9**, 378 (2022).

[32] F. Z. Yang, K. F. Luo, W. Zhang, X. Guo, W. R. Meier, H. Ni, H. X. Li, P. M. Lozano, G. Fabbris, A. H. Said, C. Nelson, T. T. Zhang, A. F. May, M. A. McGuire, R. Juneja, L. Lindsay, H. N. Lee, J. M. Zuo, M. F. Chi,

X. Dai, L. Zhao, and H. Miao, Incommensurate transverse Peierls transition (2024), arXiv:2410.10539 [cond-mat.str-el].

[33] S. R. Kotla, L. Noohinejad, P. Pokhriyal, M. Tolkiehn, H. Agarwal, S. Ramakrishnan, and S. van Smaalen, Realization of broken inversion symmetry in the charge density wave phase in $EuAl_4$ (2025), arXiv:2506.01633 [cond-mat.str-el].

[34] S. Cherifi-Hertel, C. Voulot, U. Acevedo-Salas, Y. Zhang, O. Crégut, K. D. Dorkenoo, and R. Hertel, Shedding light on non-Ising polar domain walls: Insight from second harmonic generation microscopy and polarimetry analysis, Journal of Applied Physics **129**, 081101 (2021).

[35] B. Croes, I. Gaponenko, C. Voulot, K. D. Grégut, Olivier Dorkenoo, F. Cheynis, S. Curiotto, P. Müller, F. Leroy, K. Cordero-Edwards, P. Paruch, and S. Cherifi-Hertel, Automatic ferroelectric domain pattern recognition based on the analysis of localized nonlinear optical responses assisted by machine learning, Advanced Physics Research (2022).

[36] I. Bersuker, On the origin of ferroelectricity in perovskite-type crystals, Physics Letters **20**, 589 (1966).

[37] H. Z. Cummins, Experimental studies of structurally incommensurate crystal phases, Physics Reports **185**, 211 (1990).

[38] A. Voute, M. Deutsch, A. Kalinko, F. Alabarse, J.-B. Brubach, F. Capitani, M. Chapuis, V. Ta Phuoc, R. Sopracase, and P. Roy, New high-pressure/low-temperature set-up available at the AILES beamline, Vibrational Spectroscopy **86**, 17 (2016).

[39] M. Yazdi-Rizi, P. Marsik, B. P. P. Mallett, and C. Bernhard, Anisotropy of infrared-active phonon modes in the monodomain state of tetragonal $SrTiO_3$ (110), Phys. Rev. B **95**, 024105 (2017).

[40] S. Siddique, J. L. Hart, D. Niedzielski, R. Singha, M.-G. Han, S. D. Funni, M. Colletta, M. T. Kiani, N. Schnitzer, N. L. Williams, L. F. Kourkoutis, Y. Zhu, L. M. Schoop, T. A. Arias, and J. J. Cha, Realignment and suppression of charge density waves in the rare-earth tritellurides $R\mathrm{Te}_3$ (R = La, Gd, Er), Phys. Rev. B **110**, 014111 (2024).

[41] S. Ramakrishnan, A. Schönleber, C. B. Hübschle, C. Eisele, A. M. Schaller, T. Rekis, N. H. A. Bui, F. Feulner, S. van Smaalen, B. Bag, S. Ramakrishnan, M. Tolkiehn, and C. Paulmann, Charge density wave and lock-in transitions of CuV_2S_4, Phys. Rev. B **99**, 195140 (2019).

[42] V. Goian, S. Kamba, O. Pacherová, J. Drahokoupil, L. Palatinus, M. Dušek, J. Rohlíček, M. Savinov, F. Laufek, W. Schranz, A. Fuith, M. Kachlík, K. Maca, A. Shkabko, L. Sagarna, A. Weidenkaff, and A. A. Belik, Antiferrodistortive phase transition in $EuTiO_3$, Phys. Rev. B **86**, 054112 (2012).

[43] J.-W. Kim, P. Thompson, S. Brown, P. S. Normile, J. A. Schlueter, A. Shkabko, A. Weidenkaff, and P. J. Ryan, Emergent superstructural dynamic order due to competing antiferroelectric and antiferrodistortive instabilities in bulk $EuTiO_3$, Phys. Rev. Lett. **110**, 027201 (2013).

[44] R. G. Burkovsky, I. Bronwald, D. Andronikova, B. Wehinger, M. Krisch, J. Jacobs, D. Gambetti, K. Roleder, A. Majchrowski, A. V. Filimonov, A. I. Rudskoy, S. B. Vakhrushev, and A. K. Tagantsev, Critical scattering and incommensurate phase transition in antiferroelectric $PbZrO_3$ under pressure, Scientific Reports **7**, 10.1038/srep41512 (2017).

[45] R. G. Burkovsky, I. Bronwald, D. Andronikova, G. Lityagin, J. Piecha, S.-M. Souliou, A. Majchrowski, A. Filimonov, A. Rudskoy, K. Roleder, A. Bosak, and A. Tagantsev, Triggered incommensurate transition in $PbHfO_3$, Phys. Rev. B **100**, 014107 (2019).

[46] A. Bosak, V. Svitlyk, A. Arakcheeva, R. Burkovsky, V. Diadkin, K. Roleder, and D. Chernyshov, Incommensurate crystal structure of $PbHfO_3$, Acta Crystallographica Section B **76**, 7 (2020).

[47] W. Zhong and D. Vanderbilt, Competing structural instabilities in cubic perovskites, Phys. Rev. Lett. **74**, 2587 (1995).

[48] A. K. Tagantsev, K. Vaideeswaran, S. B. Vakhrushev, A. V. Filimonov, R. G. Burkovsky, A. Shaganov, D. Andronikova, A. I. Rudskoy, A. Q. R. Baron, H. Uchiyama, D. Chernyshov, A. Bosak, Z. Ujma, K. Roleder, A. Majchrowski, J.-H. Ko, and N. Setter, The origin of antiferroelectricity in $PbZrO_3$, Nat. Commun. **4**, 2229 (2013).